Vol 17 No 7, July 2008
1674-1056/2008/17(07)/2574-06

Chinese Physics B

© 2008 Chin. Phys. Soc.
and IOP Publishing Ltd

Growth and collapse of laser-induced bubbles in glycerol–water mixtures*

Liu Xiu-Mei(刘秀梅), He Jie(贺 杰), Lu Jian(陆 建)†, and Ni Xiao-Wu(倪晓武)

Department of Applied Physics, Nanjing University of Science & Technology, Nanjing 210094, *China*

(Received 30 October 2007; revised manuscript received 24 December 2007)

Comprehensive numerical and experimental analyses of the effect of viscosity on cavitation oscillations are performed. This numerical approach is based on the Rayleigh–Plesset equation. The model predictions are compared with experimental results obtained by using a fibre-optic diagnostic technique based on optical beam deflection (OBD). The maximum and minimum bubble radii as well as the oscillation times for each oscillation cycle are determined according to the characteristic signals. It is observed that the increasing of viscosity decreases the maximum bubble radii but increases the minimum bubble radii and the oscillation time. These experimental results are consistent with numerical results.

Keywords: optical beam deflection, cavitation bubble, viscosity
PACC: 4755B

1. Introduction

Cavitation bubble, a special phenomenon of laser–matter interaction, occurs in liquids.[1−5] It plays a decisive role in a variety of practically important physical processes, from sonoluminescence, electrochemical flotation, and electric discharge in fluids to thermonuclear reactions due to high temperatures and pressures arising at the collapse of bubbles.

When a focused short laser pulse is fired into a liquid near a solid wall, it induces optical breakdown through nonlinear absorption, which leads to plasma formation in the laser's focal area. Plasma expansion is always accompanied by the emission of shock waves and the generation of cavitation bubbles.[1,6] In general, a cavity oscillates several times emitting acoustic transients at the end of each cycle, until the cavity totally dissolves in liquids.

Cavitation bubbles also exist in liquids other than water. The influence of liquid viscosity on cavitation bubble and shock waves behaviour has aroused people's interest and has been widely investigated in many fields. For example, in the field of space engineering, Tomita *et al*[7] have reported that after the high-speed cryogenic pump full of a cryogenic liquid has been driven for a long time, cavitations occur and reduce the performance of the pumps. Bhaga and Weber[8] and Hua and Lou[9] investigated the rising and the deforming of a bubble in a quiescent viscous liquid under different flow regimes. In laser medicine, Brujan[10] investigated the behaviour of a single bubble in blood.

However, few papers are concerned with the influence of viscosity on bubble radius evolution in a quiescent incompressible liquid. To this end, a glycerol–water mixture is chosen, which is an available fluid if one wants to easily vary the viscosity of a fluid over a large range. The maximum and minimum bubble radii, as well as bubble life-time in a glycerol–water mixture of increasing viscosity are studied in this paper by using an optical beam deflection technique. These experimental data are compared with the results of numerical Rayleigh–Plesset solutions.

2. Numerical technique

The radius time evolution of a spherically symmetric bubble surrounded by an incompressible and viscous fluid is described by the Rayleigh–Plesset equation[11]

$$R\ddot{R} + \frac{3}{2}\dot{R}^2 = \frac{P_{\mathrm{R}} - P_\infty}{\rho} = \frac{1}{\rho}\left(P_{\mathrm{v}} + P_{\mathrm{g}} - P_\infty - \frac{2\sigma}{R}\right) - 4\nu\frac{\dot{R}}{R}, \qquad (1)$$

*Project supported by the National Natural Science Foundation of China (Grant No 60578015), the Teaching and Research Award Program for Outstanding Young Teachers in Higher Education Institute of China (2003-2008), and the National Key Opening Experiment Foundation of Laser Technology of China (Grant No 2005).

†Corresponding author. E-mail: lujian@mail.njust.edu.cn

where P_∞ is the static pressure, P_v is the vapour pressure inside the bubble, P_g is the gas partial pressure, R is the spherical bubble radius, $\dot{R}$ is the growth speed of the bubble, $\ddot{R}$ is the accelerated speed, ρ is the density of fluid, σ is the surface tension coefficient, and ν is (kinematic) viscosity.

For large heat capacity of the surrounding liquid and small bubble mass, the heat unbalance caused by gas diffusing from the liquid into the oscillating bubble can be adjusted quickly by surrounding liquid, and the gas and its temperature in the bubble can be considered as constants. Therefore, in derivation both σ and P_v are assumed to be uniform ($\sigma = 0.072\,\mathrm{N/m}$, $P_\mathrm{v} = 2330\,\mathrm{Pa}$). As the growth or collapse rate of the bubble is very rapid, this process is assumed to be adiabatic and the gas partial pressure is given by

$$p_\mathrm{g} = p_{\mathrm{g}0}\left(\frac{R_0}{R}\right)^{3\gamma} = kp_\infty\left(\frac{R_0}{R}\right)^{3\gamma}, \quad k \in (0.1), \quad (2)$$

where γ is the radio of specific heats and taken as 1.4 in this paper, R_0 is the initial bubble radius, $p_{\mathrm{g}0}$ is the initial gas partial pressure, and k represents the proportion of gas content.

Substituting expression (2) into Eq.(1) yields

$$R\ddot{R} + \frac{3}{2}\dot{R}^2 = \frac{kP_\infty}{\rho}\left(\frac{R_0}{R}\right)^{3\gamma} - \frac{P_\infty - P_\mathrm{v}}{\rho} - 4\nu\frac{\dot{R}}{R} - \frac{2\sigma}{\rho R}. \quad (3)$$

The initial conditions are as follows: when $t = 0$, then $R = R_0$, and $\dot{R} = \ddot{R} = 0$.

The numerical simulations of the radius evolution R versus t are shown in Fig.1, which are obtained from Eq.(3).

Figure 1 illustrates the effect of viscosity on bubble oscillation. Each curve corresponds to a different viscosity. The numerical results indicate that the bubble expands or collapses less violently in a more viscous incompressible liquid. The results also show that liquid viscosity not only influences the maximum and minimum bubble radius but also bubble life-time.

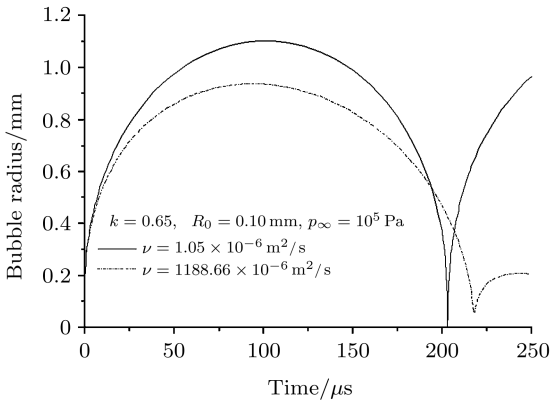


Fig.1. Numerical simulations of radius evolution R versus t with different values of viscosity.

3. Experiment

3.1. Experimental method

The experimental arrangement based on OBD is outlined in Fig.2, which was first reported in detail in Ref.[12]. A Q-switched Nd:YAG laser with a wavelength of 1.064 μm and a pulse duration of 10 ns is used to produce a single bubble. An attenuator adjusts the incident laser energy without changing its spatial distribution. Optical components 4 and 5 consist of an adjustable-focus extender lens. In order to reduce the probability of generating multiple plasmas and to keep a bubble in spherical shape, the laser pulse is expanded and collimated by this extender lens so that it has a relative large cone angle in liquid. A copper block with a plane surface is immersed in a glass cuvette full of a mixture of glycerin and water in various concentrations at room temperature 20°C (see Table 1).[13]

Table 1. Values of viscosity ν of glycerin–water mixtures in experiment.

glycerin (% by vol.)	0	20	40	60	80	100
viscosity $\nu/(10^{-6}\mathrm{m}^2\cdot\mathrm{s}^{-1})$	1.005	1.695	3.494	8.189	49.710	1188.739

In a detection region, a He–Ne laser used as a probe beam is focused close to the optical breakdown region and parallel to the boundary surface. This deflected beam is then focused into a single-mode optical fibre by using a microscope objective. This fibre serves as a position-sensitive detector and is mounted on a five-dimensional fibre-regulating stand with a 0.1 μm spatial resolution. The light from the optical fibre is then fed into a photomultiplier and recorded by using a digital oscilloscope. In order to increase the signal-to-noise ratio, a narrow-band interference filter is placed in front of the fibre. The scattered light

from each laser pulse is monitored as a trigger signal by using a photoelectric diode 17 with a rise time of 0.1 ns. Elements numbered from 9 to 14 shown in Fig.1 build up an OBD diagnostic system. This OBD part is placed on a two-dimensional platform that can be moved in the direction of the arrow with a spatial resolution of 10 μm.

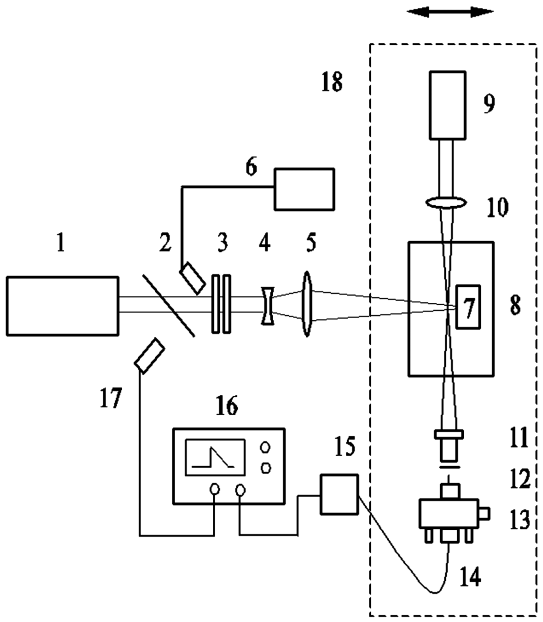


Fig.2. Diagram of experimental setup: 1, Q-switched Nd:YAG laser (1.06 μm wavelength, pulse duration 10 ns); 2, beam splitter; 3, attenuator group; 4, concave lens (f = 50 mm); 5, convex lens (f = 150 mm); 6, pyroelectric energy meter; 7, copper target; 8, glass cuvette (100 mm × 100 mm × 150 mm); 9, He-Ne laser (Power 5 mW, 0.63 μm wavelength); 10, convex lens (f = 50 mm); 11, microscope objective (20×, f = 4 mm); 12, interference filter (0.63 μm wavelength); 13, 5-axis fibre chuck positioner (0.1 μm spatial resolution); 14, single-mode optical fibre; 15, photomultiplier (Hamamatsu H5773 with 2 ns rise time); 16, digital oscilloscope (Tektronix THS730A); 17, PIN photodiode (with 0.1 ns rising edge); 18, two-dimensional platform (10 μm spatial resolution).

For optimizing the performance the optical fibre should be aligned so that the initial coupling light flux is at a maximum. One can easily do so by observing the amplitudes of the signals displayed on the oscilloscope during the alignment. In this case, any beam deflection will reduce the coupling flux. In addition, the initial zero spatial position is defined as the place where half of the probe beam is blocked by the target material. To eliminate the random error, the data collected in this paper are the average values of five experimental measurements.

3.2. Experimental results

While a bubble passes through search coverage, the refractive index of the liquid changes. As a result, the transient light flux arriving at the photomultiplier is modulated. Figure 3 is a diagram of the probe beam passing through an oscillating cavity. Figure 4 shows the characteristic profiles at the four typical detection positions (a–d) marked in Fig.3. In this figure, the applied laser energy is 30.54 mJ and the distance L from the laser focus to the boundary is 2.85 mm. The experimental criteria for judging the maximum and minimum bubble radii depend on whether the characteristic peak signals appear.

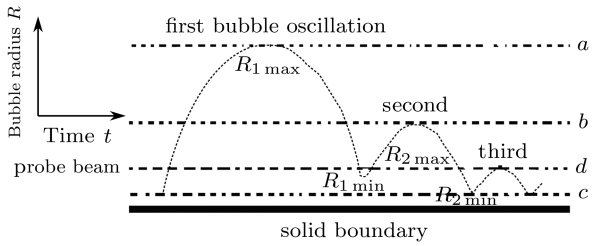


Fig.3. Schematic diagram of a probe beam passing through an oscillating cavitation bubble.

When the probe beam lies outside the maximum bubble radius $R_{\max}$, only the laser-generated plasma shock wave and collapse shock wave will appear. If the probe beam moves closer to the target, which is just inside the first maximum bubble radius as indicated at the position marked with a letter a in Fig.3, the corresponding deflection signal of the first pulsation appears as a peak signal in Fig.4(a). When the detection distance is reduced further, the refractive index gradient inside the cavitation bubble region is large enough to make the probe beam deflect completely out of the fibre core, which leads to a flat-top signal. Further decreasing the distance to the locations marked with a letter b in Fig.3, another peak signals induced by the second bubble oscillations appear as shown in Fig.4(b). Hence this distance corresponds to the second maximum radius.

If a probe beam is moved from the near field to the far field, the detected signals will be quite different from those shown above. When the probe beam is at the position marked with a letter c in Fig.3, a valley occurs on the envelope as shown in Fig.4(c), because the probe beam just passes through the minimum contracting bubble wall. At the arrival time of beam, this spatial position corresponds to the minimum radius

$R_{2\,\min}$ at the second oscillation cycle. With the detection distance increasing further, another valley occurs that corresponds to the minimum radius $R_{1\,\min}$ at the first oscillation. Furthermore, the oscillation time of the bubble can also be determined by these typical waveforms.

According to the experimental criteria mentioned above, the maximum radius $R_{\max}$, the minimum radius $R_{\min}$ and the oscillation time $T_{\rm osc}$ of the bubble during the first two oscillations in water are determined as follows: $R_{1\,\max} = 1.05\,\mathrm{mm}$ and $R_{2\,\max} = 0.51\,\mathrm{mm}$; $R_{1\,\min} = 0.13\,\mathrm{mm}$ and $R_{2\,\min} = 0.07\,\mathrm{mm}$; $T_{1\rm osc} = 180.8\,\mu\mathrm{s}$ and $T_{2\rm osc} = 107.2\,\mu\mathrm{s}$. The data indicate that the maximum and minimum bubble radii and the life-time during each oscillation all decrease sharply for successive oscillations.

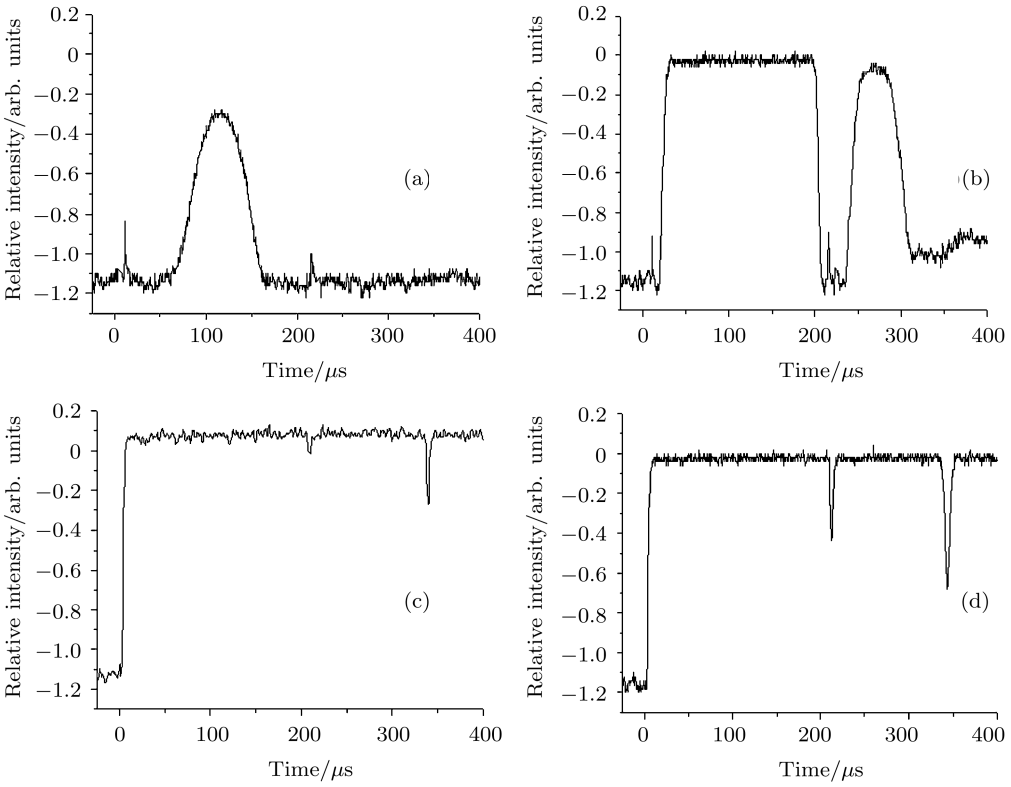


Fig.4. Characteristic signals of optical beam deflection in different stages.

3.3. Comparison between experimental results and numerical simulations

By tracking the arrival times of the bubble walls in its expanding and contracting stages at the corresponding detection distance, the temporal oscillation characteristics of a cavitation bubble oscillation near a solid boundary can be obtained. Figure 5 presents the variation of bubble radius with time, and the solid circles denote the results obtained for the bubble oscillating in water, while the open circles represent the corresponding results for pure glycerin. Here, laser pulse energy is 30.54 mJ and the corresponding non-dimensional distance γ is 2.71. There exists a large difference in bubble behaviour between water and pure

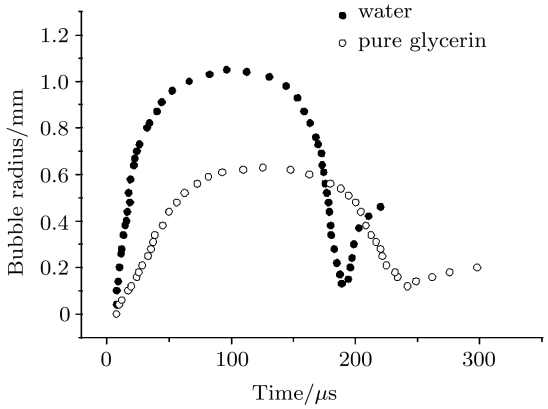


Fig.5. Radius-time relationship of a cavitation bubble as determined by using the optical beam deflection technique.

glycerin in Fig.5. It appears that the maximum bubble radius become smaller in pure glycerin. In addition, both the minimum bubble radius and bubble life-time become larger in pure glycerin.

The corresponding numerical results of bubble radius varying with time in water and pure glycerin are plotted in Fig.1. A direct comparison between experimental and numerical results shows that they are in good agreement with each other qualitatively while going into details on the influence of viscosity on bubble radius and bubble life-time. However, the present simulation considers only the viscous dissipation and neglects the surface tension variation, fluid compressibility, thermal effects, etc, and so there seems to exist a slight discrepancy between numerical and experiment results. So a more sophisticated model equation for the bubble oscillation should be developed in the future.

4. The influence of viscosity on bubble growth and collapse

Effects of viscosity on bubble dynamics are explored by monitoring radius and oscillation time versus time. Figure 6 is a logarithmic plot of the maximum bubble radius $R_{\max}$ against viscosity ν. The solid squares in Fig.6 denote the experimental results, while the solid line represents numerical results. The

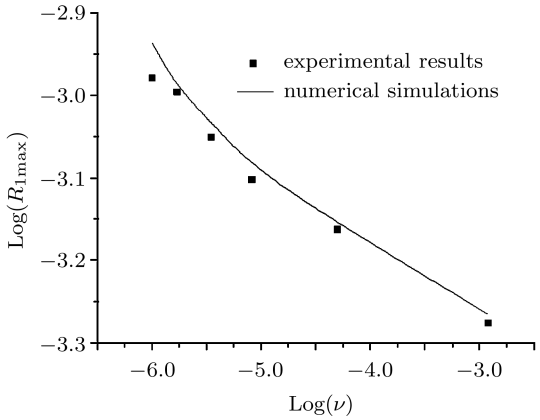


Fig.6. Logarithmic plot of the bubble maximum radius $R_{\max}$ against viscosity ν.

data indicate that the maximum bubble radius appears to decrease sharply with viscosity ν increasing, which is perhaps due to the slowing effect of viscosity on the bubble expansion. The viscosity of the fluid would exert on the bubble a radial force opposite to the attempted motion in the fluid, thereby dissipating the bubble's energy and slowing its expansion. So the gas bubble in the viscous liquid can achieve a smaller maximum radius as a result of lower bubble energy. Besides, for the maximum bubble radius there is a reasonable agreement between experimental and numerical results.

The slowing effect of the viscosity on the collapse of the bubble can also be found. Figure 7 is a logarithmic plot of the minimum bubble radius $R_{\min}$ against viscosity ν. There is a reasonable agreement between numerical results (solid line) and experimental results (solid squares). The data indicate that the minimum bubble radius increases sharply with viscosity ν increasing. As more energy is dissipated due to larger viscosity at the collapse, constriction of the bubble is not evident. So the bubble size at the final stage of every contraction is larger.

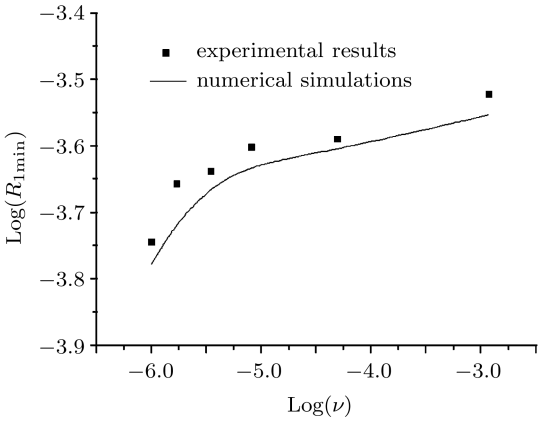


Fig.7. Logarithmic plot of the bubble minimum radius $R_{\min}$ against viscosity ν.

In Fig.8, it is shown that the oscillation time is also dependent on viscosity. The solid squares in Fig.8 denote the experimental results, while the solid line represents the corresponding numerical results. There exists a reasonable agreement between numerical and experimental results. Figure 8 shows that the oscillation time appears to increase slightly with viscosity ν increasing. Furthermore, the larger the viscosity is, the longer the oscillation time of the bubble will be. This could be another effect of viscosity on the bubble dynamics. As mentioned earlier, the viscous force decreases the growth and collapse of a bubble, making it expand or collapse less violently. That is to say, owing to the increasing of viscous drag, the oscillation time is prolonged and the impact speed is also decreased.

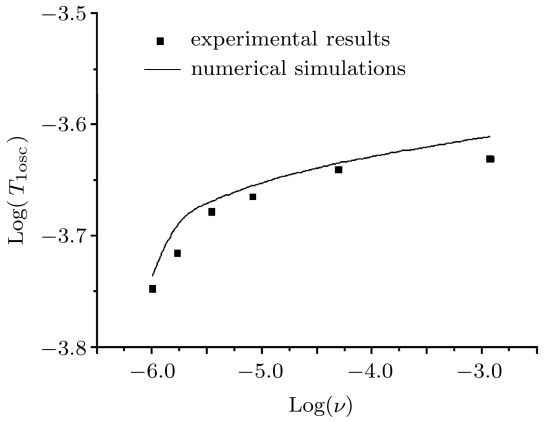


Fig.8. Logarithmic plot of the bubble life-time $T_{\rm osc}$ against viscosity ν.

5. Conclusion

The influence of viscosity on the bubble oscillation has been studied numerically and experimentally. Some interesting phenomena have been experimentally investigated by using the optical beam deflection, for instance, the maximum and minimum bubble radii at each oscillation as well as the life-time decrease sharply for successive oscillations. The experimental results also show that viscosity plays a role in dampening mechanical energy during the growth and collapse of the bubble. Increasing viscosity will both decrease the maximum bubble radius and the rates of growth and collapse, but also increase the minimum bubble radius and the bubble life-time. These experimental results are consistent with theoretical analyses.

References

[1] Vogel A, Busch S and Parlitz U 1996 *J. Acoust. Soc. Am.* **100** 148
[2] Chen X, Xu R Q, Shen Z H, Lu J and Ni X W 2004 *Chin. Phys.* **13** 505
[3] Tomita Y and Kodama T 2003 *J. Appl. Phys.* **94** 2809
[4] Lou S T, Gao J X, Xiao X D, Li X J, Li G L, Zhang Y, Li M Q, Sun J L and Hu J 2001 *Chin. Phys.* **10** 108
[5] Toegel R, Luther S and Lohse D 2006 *Phys. Rev. Lett.* **96** 114301
[6] Ohl C D, Kurz T, Geisler R, Lindau O and Lauterborn W 1999 *Phil. Trans. R. Soc. London* Ser. A **357** 269
[7] Tomita Y, Tsubota M, Nagane K and An-naka N 2000 *J. Appl. Phys.* **88** 5993
[8] Bhaga D and Weber M E 1981 *J. Fluid Mech.* **105** 61
[9] Hua J S and Lou J 2007 *J. Comput. Phys.* **222** 769
[10] Brujan E A 2000 *Europhys. Lett.* **50** 175
[11] Brennen C E 1995 *Cavitation and Bubble Dynamics* (Oxford: Oxford University Press) Chapter 2
[12] Chen X, Xu R Q, Chen J P, Shen Z H, Lu J and Ni X W 2004 *Appl. Opt.* **43** 3251
[13] Maxworthy T, Gnann C, Kurten M and Durst F 1996 *J. Fluid Mech.* **321** 421